3

Abundance of elements in Ba stars II: Analysis of Chemical abundances

3.1 Introduction

Ba stars which represent almost one percent Kovacs (1985)[162] of the total red giants so far detected were first identified as a distinct group of peculiar objects by Bidelman & Keenan (1951)[50]. These are Pop I red gaints with spectral class G to K and their spectra show strong presence of singly ionized Ba II lines, indicating an overabundance of s-process elements. The most accepted interpretation for the observed abundance patterns in barium stars is that, they acquired the enrichment of s-process nucleosynthesis from an AGB companion that later evolved to a white dwarf. Variations in radial-velocity in barium stars was revealed by McClure et al. (1980)[163] and further confirmed by McClure (1983[164], 1984[165]) and Udry et al. (1998a[166],b[167]) suggested presence of companions. Detailed abundance studies of barium stars are thus important for a better understanding of the s-process mechanisms in AGB stars, as well as the mass transfer mechanisms in binary systems. Present theories include two main types of mass transfer mechanisms for barium stars in binary systems, the Roche-lobe overflow (RLOF) and wind-accretion scenarios. In the RLOF scenario, for sufficiently close binaries containing a thermally pulsing AGB (TP-AGB) star, as the star expands past the Roche lobe the material which lies outside the lobe can fall off into the secondary object. In the wind accretion model of Boffin & Jorrisen (1988)[168], the authors have shown that for large orbital separation the contamination of Ba stars depends only upon the present value of orbital separation and mass of the white dwarf companion. Here part of matter are ejected through a wind by an AGB star and the system remain always detached. This is the more favoured channel for barium star formation. An intermediate regime in which some wind mass-transfer occurs before RLOF begins has also been suggested (Han et al. (1995)[169]). However, none of these models can explain all the physical and orbital properties of Ba stars. While RLOF scenario is not favourable as this terminates the TP-AGB and lessens the production of barium, preventing barium-star formation, the wind-accretion scenario does not explain the distribution of eccentricities and periods of barium stars (Izzard et al. (2010)[170]). Further studies are necessary to have clearer pictures on these issues. As much insight about the origin and evolution of heavy elements and the evolved AGB companion can be obtained from the chemical composition studies of these objects, and, given the current number of abundance analyses available, (although gradually increasing but for limited number of heavy elements), detailed abundance studies of even one or two more objects represent a significant contribution. In the present work we have undertaken to conduct a detailed chemical composition study for four peculiar stars listed in the barium stars catalogue of Lü (1991)[146], based on high resolution spectra (R $\sim$ 42000) and high S/N with $>$ 100 at about 5500 Å. Among these four stars considered here namely(HD-49641,HD-58368,HD-119650 and HD-191010) two objects HD-49641 and HD-58368 are included in the list of 'Certain Ba II stars' and one object HD-119650 is included in the list of 'Marginal Ba II stars' of MacConnell et al. (1972)[171].

3.2 Earlier studies on HD-49641 and HD-58368:

No detailed studies were available in literature for these objects until recently when these two objects, HD-49641 and HD-58368 are found to be included in the chemical composition studies of barium stars by Yang et al. (2016)[172] and de Castro et al. (2016)[173]. But Yang et al. (2016)[172] have reported abundances for five heavy elements (Y, Zr, Ba, La and Eu) and de Castro et al. (2016)[173] have also reported on abundances of five heavy elements (Y, Zr, La, Ce, Nd) whereas our study covers the abundance analysis of eleven neutron-capture elements and compared and contrast our results for these two objects with the results of the above two studies whenever possible.

Yang et al. (2016)**[172]**:

These two objects were included in their chemical abundance studies of 19 barium stars. They have determined the stellar atmospheric parameters using red spectra in the wavelength range $5500-9000$ Å with a resolution R $\sim$30,000 and S/N $\geq$60. The derived T_{eff} obtained using color indices (B$-$V) and the empirical calibration of Alonso et al. (1999[155], 2001[174]) for giant stars are lower than our estimates by 350 K in case of HD-49641 and by 318 K in case of HD-58368. Their lower values are likely due to the fact that the color (B$-$V) is affected by CN and C_2, making the stars redder and as a result the temperature derived from this color may be lower (Allen & Barbuy 2006[51]). Estimated log g obtained by them using

Hipparcos parallaxes also differ significantly from our estimates. The chemical abundance estimates of Na, Al, α- and iron-peak elements (O, Na, Mg, Al, Si, Ca, Sc, Ti, V, Cr, Mn, Ni) of Yang et. al(2016)[172] are found to be similar to the solar abundances. Overabundances of neutron-capture process elements relative to the Sun are noticed in both the stars. The Y I and Zr I abundances are lower than Ba, La and Eu, but higher than the α- and Fe-peak elements. The authors noted a positive correlation between Ba intensity and [Ba/Fe] in their sample of stars. For the n-capture elements (Y, Zr, Ba, La), there is an anti-correlation between their [X/Fe] and [Fe/H]. With [Ba/Fe]= 1.13 and 0.98 respectively for HD49641 and HD-58368, they have confirmed these objects to be strongly enhanced barium stars.

de Castro et al. (2016)**[173]**:

In this work the authors have presented a homogeneous analysis of photospheric abundances based on high-resolution spectroscopy of a sample of 182 barium stars and candidates. HD-49641 and HD-58368 are two members of this extended sample. The methodology employed by these authors to derive the stellar parameters are similar to ours. However, there lies significant differences between ours and their estimates of stellar atmospheric parameters, T_{eff} and surface gravity log g. While de Castro et al. (2016)[173]'s estimates for temperature and log g for HD-49641 are 4400 K and 1.5 respectively our estimates are significanltly higher with values 4700 K and 3.4. Their estimates of the abundances of α-elements and iron peak elements are similar to those of field giants with the same metallicity. The observed enrichment in sodium is attributed to the operation of Ne-Na cycle. These two stars are also found to exhibit overabundance of the elements created by the s-process. From the measurements of the mean heavy-element abundance pattern as given by the ratio [s/Fe], it was found that the barium stars present several degrees of enrichment. From the measured photospheric abundances of the Ba-peak and the Zr-peak elements, [s/Fe] and the [hs/ls] ratios (where hs refers to heavy s-process elements and ls refers to light s-process elements) are found to be strongly anticorrelated with the metallicity, and that, the barium stars follow an age–metallicity relation.

3.3 Linelist, Equivalent widths and Abundance analysis

Abundances for most of the elements are determined from the measured equivalent widths of lines presented in Appendix B due to neutral and ionized elements using a recent version of MOOG of Sneden (1973)[157] and the adopted model atmospheres. From a close comparison of the spectra of the programme stars with that of the spectrum of Arcturus a line list of all the elements was generated. However, only the lines that were used for abundance analysis are included in the line list; others being blended with contributions from other species could not be used for abundance analysis. The primary source of the adopted log gf values for the atomic lines due to these elements is Kurucz atomic line database (Kurucz 1995a[178], b[179]) other sources from literature, such as, Karinkuzhi & Goswami (2014[156], 2015[180]), Goswami & Aoki (2010)[181], Aoki et al. (2005[182], 2007[183]), Goswami et al. (2006[43], 2016[184]), Jonsell et al. (2006)[185], Sneden et al. (1996)[186], Luck and Bond (1991)[187] were also consulted. For the elements Sc, V, Mn, Ba, La and Eu, spectrum synthesis calculation considering hyperfine structure is used to find the abundances. The line list for each region synthesised is taken from Kurucz atomic line list (http://www.cfa.harvard.edu/amdata/ampdata/kurucz23/sekur.html). For a few La lines the log gf values are taken from Lawler et al. (2001)[188]. We had also estimated the Fe abundances considering our line-list given in Appendix A and using stellar atmospheric models corresponding to the stellar parameters of Yang et al. (2016)[172] for the two objects HD 49641 and HD 58368. In either case we did not arrive at the desired zero slope for 'abundance vs excitation potential' plot and 'abundance vs equivalent width' plot. We have therefore adopted the stellar parameters estimated by us in determining the abundances of the elements. Derived abundance values along with the abundance ratios with respect to iron are listed in Tables 3.2. To examine the accuracy of our estimates we have also measured on solar spectra the equivalent widths for a large number of lines (these lines are also detected in the spectra of our programme stars) and measured the solar abundances using the log gf values that we have adopted. The solar atmospheric parameters used are microturbulent velocity 1.25 kms^{-1}, T$_{eff}$ = 5835 K and log g = 4.55 cm s^{-2}. When comparing with Asplund et al. (2009)[177], the derived abundances are found to match closely within a range of 0.08 $-$ 0.1 dex. A comparison of our estimated abundance ratios for elements Na to Zn with respect to Fe, with their counterparts in normal giants and Ba stars obtained from literature are shown in Fig. 3.6 (upper left and right panels). We have illustrated a few examples of spectrum synthesis calculations for Y (Fig. 3.1), Ba (Fig. 3.2, left panel) and La (Fig. 3.2, right panel). In Table 3.1, we have presented [ls/Fe], [hs/Fe] and [hs/ls] values, where ls represents the light s-process elements Sr, Y and Zr and hs represents the heavy s-process elements Ba, La, Ce, Nd and Sm. A comparison of our estimated abundance ratios for neutron-capture elements with their counterparts in normal giants and Ba stars obtained from literature are shown in Fig. 3.3 (lower left and right panels).

3.4 Discussion on indivisual elemental abundance

3.4.1 Na and Al

Sodium (Na): Na abundance for all the programme stars using the lines at 5682.65 and 5688.22 Å whenever available. The object HD 191010 shows a marginally higher abundance ratio with [Na/Fe]= 0.59 than those observed in normal giants (Fig. 3.6, upper right panel). Many barium stars studied by de Castro et al. (2016)[55] also show sodium abundance ratios [Na/Fe] in the range 0.3 – 0.6. Sodium does not show any trend with metallicities in field giants. Two of our objects HD 58368 and HD 119650 show sodium abundances similar to many field giants with [Na/Fe] values 0.22 and 0.24, respectively. The object HD 49641 however shows a mild underabundance with [Na/Fe]= -0.19 which is somewhat similar to that obtained for the object HD 203137 ([Na/Fe] = -0.14) as reported by Yang et al. (2016)[172].

Aluminium (Al): We could not estimate Al abundance as no clear Al lines could be detected due to line blending.

3.4.2 Mg, Si, Ca, Sc, Ti, V

α-elements in field giants are known to show a slight increase with decreasing metallicity. Following are the estimations of observed abundances in our study related to our sample of stars.

Magnesium (Mg): Three stars in our sample except HD 191010 (Tables 3.2) exhibit abundance ratios of Mg, lower than that generally seen in normal giants. While HD 191010 is found to show a near solar value our estimates for the other three objects are -0.41, -0.39 and -0.16 respectively for HD 49641, HD 58368 and HD 119650. Thus our estimated values are however well within the range normally seen in barium stars. This is not surprising as some barium stars are known to exhibit underabundance (Yang et al. (2016)[172]) estimated a ratio of [Mg/Fe] ~ -0.28 for the two barium stars HD 31308 and HD 224276). Yang et al. (2016)[172] and de Castro et al. (2016)[55] estimated [Mg/Fe] = -0.13 and -0.03 respectively for HD 58368.

Silicon (Si): In all the four stars Si abundance is found to be lower than what is normally observed in barium stars and normal giants. Further studies including theoretical aspects would be worthwhile to understand these anomalies.

Calcium (Ca): The behaviour of Ca is found to be similar as seen generally in normal giants with none of our sample overabundant in Ca.

Scandinium (Sc): While Sc abundance ratios in three stars are similar to those observed in normal giants, HD 49641 shows a higher value with [Sc/Fe] = 0.47. Sc abundance ratios are well within the range seen in barium stars. The abundance ratio of V in HD 119650 is marginally higher ([V/Fe] = 0.52) than those seen in normal giants. The Sc abundance is estimated using the Sc II line at 6245.63 Å considering hyperfine structure from Prochaska & McWilliam (2000)[189].

Titanium (Ti): Abundance ratios of Ti with respect to iron are similar to those generally observed in normal giants and barium stars.

Vanadium (V): Although abundance of V is calculated using measured equivalent widths for many lines, this being an odd Z element its abundance is also estimated from spectrum synthesis calculation of V I line at 5727.028 Å taking into account the hyperfine components from Kurucz database. The values obtained from spectrum synthesis calculations are listed in the abundance tables.

3.4.3 Cr, Mn, Co, Ni, Zn

Abundance ratios of iron peak elements exhibit similar values as seen in barium stars. However, a close agreement with the values of normal giants are not observed in all the cases.

Cromium (Cr): Cr abundances derived using Cr I lines show near solar values for HD 119650 (+0.06) and HD 191010 (-0.11). Cr is overabundant in HD 49641 with [Cr/Fe] = 0.44 and underabundant in HD 58368 with [Cr/Fe] = -0.32. Cr abundances measured using Cr II lines whenever possible also give similar results.

Manganese (Mn): Mn abundance is obtained using spectrum synthesis calculation of 6013.51 Å line taking into account the hyperfine structures from Prochaska & McWilliam (2000)[189]. All the four sample stars are found to be slightly underabundant with -0.27$\leq$ [Mn/Fe]$\leq$ -0.15.

Cobalt (Co): Except for HD 58368 and HD 119650, with [Co/Fe] $\sim$ 0.27 and 0.15 the other stars in our sample show near-solar values or mild underabundance for cobalt (Co).

Nickel (Ni): Abundances of nickel (Ni) measured from Ni I lines give near-solar values for HD 58368. HD 49641 show overabundance with [Co/Fe] with value 0.35. However the other two HD 119650 and HD 191010 show underabundance with value -0.05 and -0.19 respectively.

Zinc (Zn): We could estimate Zn abundance only in two stars, HD 58368 and HD 119650 using a single Zn I line at 4722.15 Å. This line returns a value [Zn/Fe] = 0.71 and 0.39 for HD 58368 and HD 119650 respectively which are higher than those normally seen in normal giants and barium stars (Fig. 3.3).

3.4.4 Sr, Y, Zr

We have also derived few light s-process elements using equivalent width measurements for their abundance determination.

Strontium (Sr): We have estimated the abundance of Sr using the Sr I line at 4607.327 Å. Sr is overabundant in all the four stars with [Sr/Fe] values 0.97, 1.19, 1.01 and 1.36 for HD 49641, HD 58368, HD 119650 and HD 191010 respectively. None of the Sr II lines detected in the spectra are found suitable for abundance estimate.

Yttrium (Y): We could measure the abundance of Y in all the four stars. Y is found to be significantly overabundant in HD 49641. We have performed spectrum synthesis calculation for three Y II lines at 5289.815, 5544.615 and 5546.009 Å for the object HD 49641 (Fig. 3.1). Two alternative synthetic spectra at the adopted value + 0.3 and -0.3 are found to demonstrate the sensitivity of the line strength to the abundances. An Y abundance of 3.50 gives satisfactory fits for the lines of Y II at 5289.815 and 5544.615 Å giving [Y/Fe] = 1.31. In Table 3.3, we have listed this value. The Y II line at 5546.009 Å can be fitted with a slightly higher abundance 4.15 that gives [Y/Fe] = 1.96. However, this line is blended with a line due to vanadium. Estimated [Y/Fe] values are 1.12, 0.68 and 0.11 in HD 58368, HD 119650 and HD 191010 respectively. Yang et al. (2016)[172] have reported abundances for

Y for HD 49641 and HD 58368 as [Y/Fe]= 0.35, 0.41 respectively. Whereas in the work of de Castro et al. (2016)[55] the values for [Y/Fe] published as 0.89, 0.85 for HD 49641 and HD 58368 respectively.

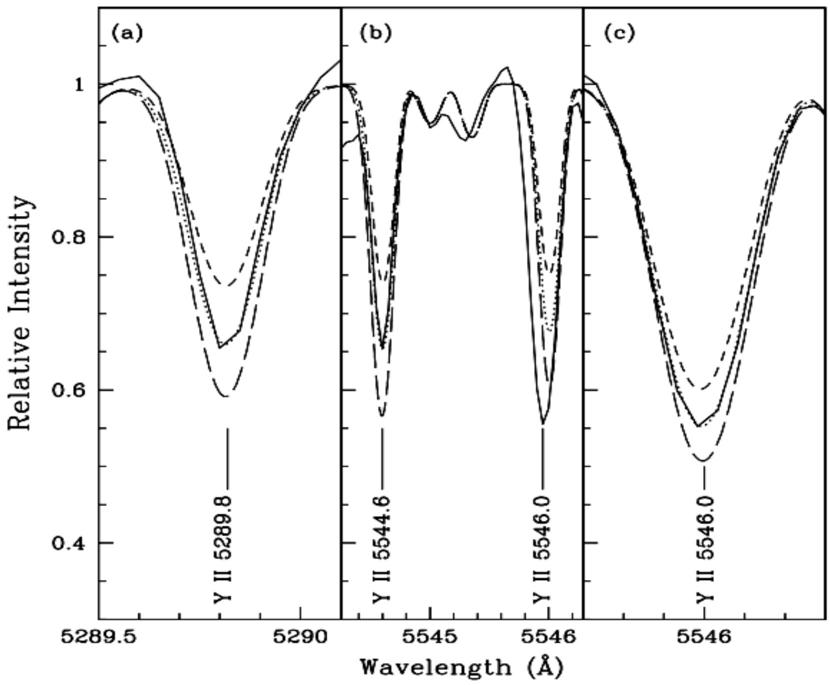

Fig. 3.1 Spectral-synthesis fits of Y II line. The dotted lines indicate the synthesized spectra and the solid lines indicate the observed line profiles. We could get good fits using the adopted value of the corresponding elements (Table 3.3).

Zirconium (Zr): Yang et al. (2016)[172] and de Castro et al. (2016)[55] have reported abundances for Zr as well.These values for HD 49641 and HD 58368 are respectively (Zr: 0.41, 0.25; Yang et al. (2016)[172] and (Zr: 0.53, 0.60; de Castro et al. (2016)[55]). However we could derive Zr abundance for three objects from Zr I lines. HD 49641 and HD 58368 both show an overabundance with [Zr/Fe] = 0.73. HD 119650 also show a mild enhancement with a value of [Zr/Fe] = 0.42. Zr abundance could not be estimated for HD 191010.

3.4.5 Ba, La, Ce, Pr, Nd, Sm, Eu, Dy

Many lines due to Ce, Pr, Nd, Sm and Dy have been measured on our spectra, the standard abundance determination method using equivalent width measurements are used for the abundance determination of the elements Ce, Pr, Nd, Sm and Dy. However we could estimate abundances of these elements in all the stars except for HD 49641 where abundances of Sm and Dy could not be estimated. Spectrum synthesis calculation are carried out for Ba, La and Eu.

Barium (Ba): We have determined Ba abundances by synthesising Ba II line at 5853.67 Å considering hyperfine components from McWilliam (1998)[190]. Two alternative synthetic spectra at the (adopted value +0.3) and (adopted value -0.3) are also have derived to demonstrate the sensitivity of the line strength to the abundances. HD 49641 and HD 58368 show over abundance of Ba with [Ba/Fe] $\geq$ 1.0, also reported in the estimation due to Yang et al. (2016)[172] as [Ba/Fe]= 1.13 and 0.98 for HD 49641 and HD 58368 respectively, which is higher than that generally noticed in normal giants. Whereas as HD 119650 and HD 191010 have been found to show Ba abundance as 0.52 and 0.40 respectively.

Lanthanum (La): La abundance for the programme stars have been derived from spectrum synthesis calculation of La II line at 4921.77 Å considering hyperfine components from Jonsell et al. (2006)[185]. Two alternative synthetic spectra at the (adopted value +0.3) and (adopted value -0.3) are also have derived to demonstrate the sensitivity of the line strength to the abundances. Except for HD 191010, La in all other stars is found to be overabundant relative to Fe with [La/Fe] $\geq$ 1.00. HD 191010 shows a mild overabundance of [La/Fe]=0.42. Estimates on La can also be found in other studies performed by Yang et al. (2016)[172] [La/Fe] = 1.38 and 1.07 for HD 49641 and HD 58368 respectively. de Castro et al. (2016)[55] as well have found overabundance of La in these two stars as 1.86 and 1.13 for HD 49641 and HD 58368 respectively.

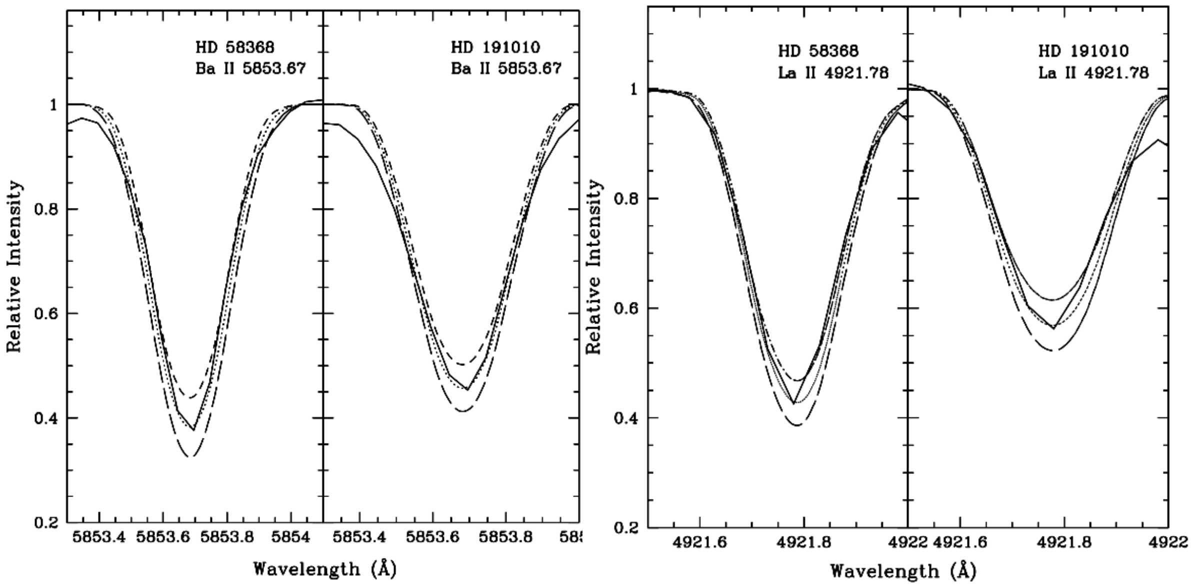

Fig. 3.2 Spectral-synthesis fits of Ba II line at 5853.6 Å (left) and La II line at 4921.77 Å (right) are shown for two objects HD 58368 and HD 191010. The dotted lines indicate the synthesized spectra and the solid lines indicate the observed line profiles.

Cerium (Ce): We have derived Ce abundance for all the programme stars using equivalent width measurements. Two of our sample HD 49641 and HD 58368 are overabundant with [Ce/Fe]$\geq$ 1.00 and the other two have this value $\geq$ 0.40.

Praseodymium (Pr): We could derive Pr abundance in the programme stars mainly using the Pr II line at 5292.619 Å. A mild over enhancement of Pr is seen in HD 119650, HD 191010 with [Pr/Fe] $\sim$ 0.53, 0.43 repectively. However HD 49641 and HD 58368 are found to be overabundant with [Pr/Fe] $\geq\sim$ 1.00.

Neodymium (Nd): Nd too have been measured on our spectra, the standard abundance determination method using equivalent width measurements are used for abundance estimates. HD 49641 and HD 58368 show mild overabundance with [Nd/Fe]= 0.40 and 0.12 respectively. On the other hand HD 119650 and HD 191010 are found to have slight overabundance in respect to [Nd/Fe] which is $\geq$ 0.90.

Samarium (Sm): Except for HD 49641, we have derived the Sm abundance using equivalent width measurements for the other three stars. And it has shown some variation in our sample. HD 58368 show overabundance with [Nd/Fe]= 1.01 as like HD 119650 with Nd bearing abundance 1.29. On the other hand HD 191010 is found to be underabundant having an abundance value -0.18.

Europium (Eu): Eu abundance is determined from spectrum synthesis calculation of Eu II line at 6645.130 Å by considering the hyperfine components from Worley et al. (2013)[191]. Our estimates of Eu abundance on HD 49641 has been found out to be overabundant with value 0.90 which is significantly different than the estimate due to Yang et al. (2016)[172] as 0.64. Other two namely HD 58368 and HD 119650 have been mildly overabundant with [Eu/Fe]$\sim$ 0.45 (0.41 reported by Yang et al. (2016)[172]) and 0.38 respectively whereas the last one of our sample is slightly overabundant having a value 0.08.

Dysprosium (Dy): We could derive Dy abundance for four objects using the Dy II lines at 4103.310 Å and 4923.167 Å. Except HD 49641 all the other three stars have shown overabundance in [Dy/Fe]$\geq$ 1.00. HD 58368 have shown large overabundance with a value 1.95. As can be seen from Table 3.3, for a few elements our estimates are significantly different from Yang et al. (2016)[172], de Castro et al. (2016)[55]. However the common trend observed is that the heavy elements in the barium stars are known to show large scatter with respect to metallicity just like in normal giants. In Table 3.1, we have presented [ls/Fe], [hs/Fe] and [hs/ls] values, where ls represents the light s-process elements Sr, Y and Zr and hs represents the heavy s-process elements Ba, La, Ce, Nd and Sm.

Table 3.1 Observed values for [Fe/H], [ls/Fe], [hs/Fe] and [hs/ls]

Star Name	[Fe/H]	[ls/Fe]	[hs/Fe]	[hs/ls]
HD 49641	−0.05	1.33	1.49	0.16
HD 58368	0.09	1.01	1.18	0.17
HD 119650	0.04	0.70	0.78	0.08
HD 191010	0.13	0.74	0.24	−0.50

The next four panel of the Fig. 3.3 shows a comparative view of the abundance pattern for light and heavy elements of our stars (from Table 3.2 & 3.3) with the data obtained from literature. In the top left upper panel, our programme stars (filled triangles) are compared with the abundance ratios observed in Ba stars (filled circles) from the literature (i.e. Zacs (1994)[192]; Liang et al. (2003)[193]; Allen & Barbuy (2006)[51, 52]; Smiljanic et al. (2007)[194]; de Castro et al. (2016)[55]). Top right panel, our programme stars (filled triangles) are compared with the abundance ratios observed in giants (filled squares) from the literature (i.e. Mishenina et al. (2006)[195]; Luck & Heiter (2007)[196]). Bottom left panel heavy elements observed in the programme stars(filled triangles) with respect to metallicity [Fe/H]. Filled circles represent Ba stars from the literature(i.e. Zacs (1994)[192]; Liang et al. (2003)[193]; Allen & Barbuy (2006)[51, 52]; de Castro et al.(2016)[55]). de Castro et al. (2016)[55]'s data are available only for five heavy elements, Y, Zr, La, Ce and Nd. Botton right panel filled squares represent normal giants from the literature (Tautvaisiene et al. (2000)[197]; Luck & Heiter (2007)[196]; Van der Swaelmen et al. (2016)[198]) our objects are indicated with filled triangles.

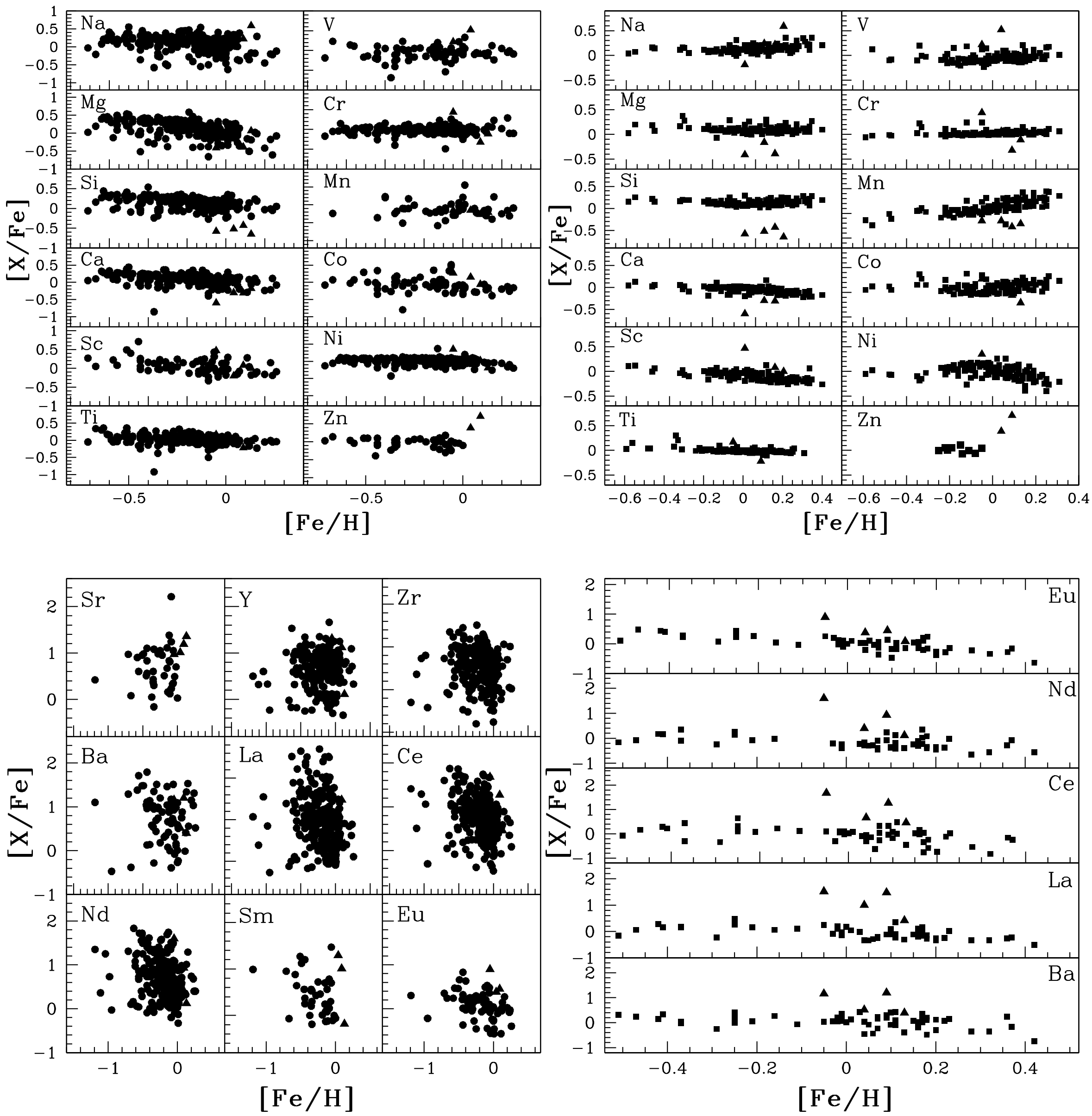

Fig. 3.3 Abundance ratios of **light** and **heavy** elements observed in the programme stars with respect to [Fe/H].

Table 3.2 Abundances of light & heavy elements in HD 49641, HD 58368, HD 119650 and HD 191010

			HD 49641			HD 58368			HD 119650			HD 191010		
Element	Z	$log\epsilon_{\odot}$	$log\epsilon$	[X/H]	[X/Fe]	$log\epsilon$	[X/H]	[X/Fe]	$log\epsilon$	[X/H]	[X/Fe]	$log\epsilon$	[X/H]	[X/Fe]
Na I	11	6.24	6.00±0.20	-0.24	-0.19	6.55±0.15	+0.31	+0.22	6.52±0.30	+0.28	+0.24	6.96±0.20	+0.72	+0.59
Mg I	12	7.60	7.14±0.07	-0.46	-0.41	7.39±0.11	-0.30	-0.39	7.48±0.07	-0.12	-0.16	7.79±0.08	+0.19	+0.06
Si I	14	7.51	6.88±0.06	-0.63	-0.58	7.17±0.19	-0.34	-0.43	7.03±0.17	-0.48	-0.52	6.99±0.20	-0.52	-0.65
Ca I	20	6.34	5.69±0.20	-0.65	-0.60	6.12±0.12	-0.22	-0.31	6.08±0.19	-0.26	-0.30	6.29±0.12	-0.05	-0.18
Sc II	21	3.15	3.70±0.20	+0.45	+0.47	3.35±0.20	+0.20	+0.08	3.25±0.20	-0.10	-0.20	3.27±0.20	+0.12	+0.00
Ti I	22	4.95	5.07±0.14	+0.12	+0.17	4.82±0.16	-0.13	-0.22	4.97±0.17	-0.02	-0.06	4.85±0.15	+0.10	-0.03
Ti II	22	4.95	–	–	–	5.08±0.01	+0.13	+0.04	5.12±0.18	+0.17	+0.07	5.30±0.07	+0.35	+0.23
V I	23	3.93	4.10±0.20	+0.17	+0.22	3.92±0.20	-0.01	-0.10	4.49±0.20	+0.56	+0.52	3.95±0.20	-0.02	-0.15
Cr I	24	5.64	6.03±0.18	+0.39	+0.44	5.41±0.11	-0.23	-0.32	5.74±0.21	+0.10	+0.06	5.66±0.19	+0.02	-0.11
Mn I	25	5.43	5.23±0.20	-0.20	-0.15	5.25±0.20	-0.18	-0.27	5.32±0.11	-0.11	-0.15	5.25±0.20	-0.18	-0.21
Fe I	26	7.50	7.45±0.13	-0.05	–	7.59±0.12	+0.09	–	7.54±0.20	+0.04	–	7.63±0.13	+0.13	–
Fe II	26	7.50	7.48±0.30	-0.02	–	7.62±0.11	+0.12	–	7.60±0.20	+0.10	–	7.62±0.12	+0.12	–
Co I	27	4.99	5.21±0.13	+0.22	+0.27	5.04±0.17	+0.05	-0.06	5.18±0.16	+0.19	+0.15	4.91±0.15	-0.08	-0.21
Ni I	28	6.22	6.52±0.18	+0.30	+0.35	6.33±0.13	+0.11	+0.02	6.21±0.13	-0.01	-0.05	6.16±0.14	-0.06	-0.19
Zn I	30	2.58	–	–	–	5.36±0.20	+0.80	+0.71	4.99±0.20	+0.43	+0.39	–	–	–
Sr I	38	2.87	3.79±0.20	+0.92	+0.97	4.15±0.20	+1.28	+1.19	3.92±0.20	+1.05	+1.01	4.36±0.20	+1.49	+1.36
Y II	39	2.21	3.50±0.20	+1.29	+1.31	3.45±0.04	+1.24	+1.12	2.99±0.18	+0.78	+0.68	2.54±0.15	+0.23	+0.11
Zr I	40	2.58	3.29±0.20	+0.71	+0.73	3.40±0.07	+0.82	+0.73	3.04±0.20	+0.46	+0.42	–	–	–
Ba II	56	2.18	3.32±0.20	+1.14	+1.16	3.50±0.20	+1.32	+1.20	2.80±0.20	+0.62	+0.52	2.70±0.20	+0.52	+0.40
La II	57	1.10	2.60±0.20	+1.50	+1.52	2.70±0.20	+1.60	+1.48	2.20±0.20	+1.10	+1.00	1.64±0.20	+0.54	+0.42
Ce II	58	1.58	3.24±0.04	+1.66	+1.68	2.97±0.07	+1.39	+1.27	2.35±0.10	+0.77	+0.67	2.16±0.06	+0.58	+0.46
Pr II	59	0.72	2.42±0.08	+1.70	+1.72	1.83±0.12	+1.11	+0.99	1.41±0.20	+0.69	+0.59	1.40±0.20	+0.68	+0.52
Nd II	60	1.42	3.00±0.12	+1.58	+1.60	2.47±0.17	+1.05	+0.93	1.92±0.09	+0.50	+0.40	1.66±0.09	+0.24	+0.12
Sm II	62	0.96	–	–	–	2.09±0.20	+1.13	+1.01	2.35±0.13	+1.39	+1.29	0.90±0.20	-0.06	-0.18
Eu II	63	0.52	1.40±0.20	+0.88	+0.90	0.99±0.20	+0.57	+0.45	1.00±0.20	+0.48	+0.38	0.72±0.20	+0.20	+0.08
Dy II	66	1.10	–	–	–	3.17±0.20	+2.07	+1.95	2.74±0.09	+1.64	+1.54	2.31±0.20	+1.21	+1.09

Table 3.3 Comparison with the literature values

starname	T_{eff}	logg	[Fe/H]	[Na/Fe]	[Mg/Fe]	[Si/Fe]	[Ca/Fe]	[Sc/Fe]	[Ti/Fe]	[V/Fe]	[Cr/Fe]	[Mn/Fe]	[Co/Fe]	[Ni/Fe]	ref
HD49641	4700	3.4	-0.05	-0.19	-0.41	-0.58	-0.60	+0.47	+0.17	+0.22	+0.44	-0.15	+0.27	+0.35	1
	4351	1.05	-0.32	-0.03	+0.49	+0.40	+0.21	+0.07	+0.04	-0.02	+0.17	+0.20	-	+0.03	2
	4400	1.5	-0.30	+0.24	+0.10	+0.22	+0.07	-	-0.02	-	+0.04	-	-	+0.05	3
HD58368	5095	3.45	+0.09	+0.22	-0.39	-0.43	-0.31	+0.08	-0.22	-0.10	-0.32	-0.27	-0.06	+0.02	1
	4777	2.47	-0.11	+0.24	-0.03	+0.27	-0.08	+0.09	-0.18	-0.35	-0.04	-0.02	-	+0.02	2
	5000	2.6	+0.04	+0.11	-0.13	+0.12	+0.06	-	-0.01	-	-0.04	-	-	+0.02	3

starname	T_{eff}	logg	[Fe/H]	[Sr/Fe]	[Y/Fe]	[Zr/Fe]	[Ba/Fe]	[La/Fe]	[Ce/Fe]	[Pr/Fe]	[Nd/Fe]	[Sm/Fe]	[Eu/Fe]	[Dy/Fe]	ref
HD49641	4700	3.4	-0.05	0.97	+2.29	0.73	1.16	1.52	1.68	1.72	1.60	-	+0.90	-	1
	4351	1.05	-0.32	-	0.35	0.45	1.13	1.38	-	-	-	-	0.64	-	2
	4400	1.5	-0.30	-	0.89	0.53	-	1.86	1.04	-	1.14	-	-	-	3
HD58368	5095	3.45	+0.09	1.19	1.12	0.73	1.20	1.48	1.27	0.99	0.93	1.01	0.45	1.95	1
	4777	2.47	-0.11	-	0.14	0.25	0.98	1.07	-	-	-	-	0.41	-	2
	5000	2.6	+0.04	-	0.85	0.60	-	1.13	0.86	-	0.69	-	-	-	3

1. Our work; 2. Yang et al.(2016)[172]; 3. de Castro et al.(2016)[55]

3.5 Stellar masses

We have derived the masses of the programme stars from their locations in the H-R diagram, using the Girardi et al. (2000)[149] data base of evolutionary tracks and our estimates of log ($L/L_\odot$) and T_{eff} (Fig. 3.4). While log ($L/L_\odot$) is derived by photometric methods using the parallax values from the Hipparcos catalogue (van Leeuwen (2007)[199]); for T_{eff} we have used our spectroscopic estimates. We have selected evolutionary tracks with initial compositions, Z = 0.019 and Y = 0.273, where Z is initial metallicity and Y is initial helium abundance. The approximated masses derived for the programme stars are presented in Table 3.4. It is to be noted that these mass estimates are only indicative as the Hipparcos parallaxes for these four objects have large uncertainty in measurements that amounts to ∼35-43% for three stars and the largest uncertainty showing for HD 119650 with ∼ 75%.

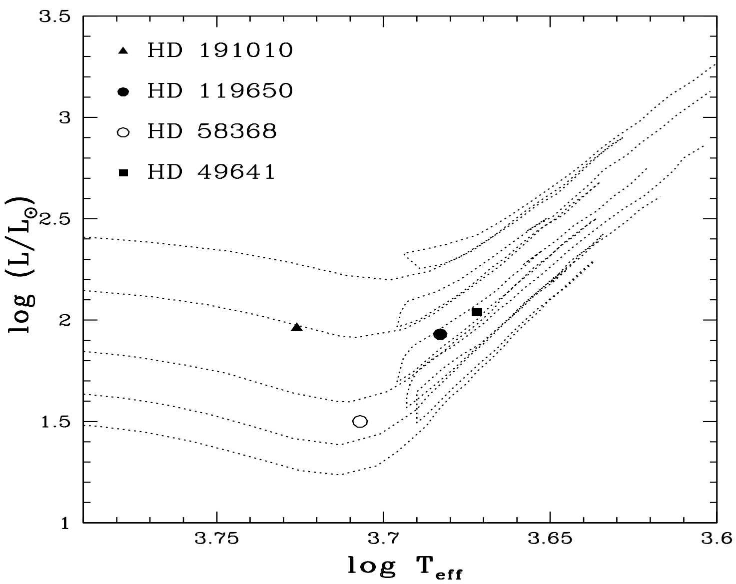

Fig. 3.4 The locations of HD 49641, HD 58368, HD 119650 and HD 191010 are indicated in the H-R diagram. The masses are derived using the evolutionary tracks of Girardi et al. (2000)[149]. The evolutionary tracks are shown for masses 2.0, 2.2, 2.5, 3.0 and 3.5 $M_\odot$ from bottom to top.

3.6 Parametric model based study

Identification of major processes contributing to the elemental abundances is likely to provide clues to the nucleosynthetic mechanisms which in turn can give clues to their evolutionary phases. In solar system both s- and r-process have contributed to the heavy elements' abundances but a significant amount of efforts have been made with s-process. The model created by Howard et al. (1986)[159], which uses an exponential distribution of neutron exposures (which will vary from time to time) via sequential irradiations, could reproduce the observed solar system σN curve, where σ is the neutron-capture cross-section and N is the abundance of the elements. Aoki et al. (2001)[161] and Zhang et al. (2006)[160] used the same model to study the observed abundances in metal-poor stars and double enhancement in metal-poor stars respectively. We have also conducted a parametric model based study to understand the contribution of these neutron-capture processes to the observed abundances of the programme stars. The s-process and the r-process are mainly responsible for producing elements heavier than iron. But the relative contributions from s- and/or r-process nucleosynthesis can not be obtained from the observed abundance of heavy elements which have been estimated using model atmospheres and spectral synthesis techniques. So identification of the process which contributes more to the abundance of heavy elements in star is important as it can give clues to their evolutionary history. In our work too, we have investigated ways to delineate the observed abundances into their respective r- and s-process contributions in the framework of a parametric model using an appropriate model function. The origin of the neutron-capture elements is explored by comparing the

Table 3.4 Derived Masses ($M_\odot$) of programme stars

Object	log ($L/L_\odot$)	log(T_{eff})	Mass(in $M_\odot$)
HD 49641	2.04	3.67	2.5
HD 58368	1.50	3.70	2.3
HD 119650	1.93	3.68	2.5
HD 191010	1.96	3.73	3.0

observed abundances with predicted s- and r-process contributions following Goswami et al. (2010)[181], (and references there in). The i_{th} element abundance can be calculated as $N_i(Z) = A_s N_{is} + A_r N_{ir} 10^{[Fe/H]}$ where Z is the metallicity of the star, N_{is} indicates the abundance from s-process in AGB star, N_{ir} indicates the abundance from r-process; A_s indicates the component coefficient that correspond to contributions from the s-process and A_r indicates the component coefficient that correspond to contributions from the r-process. We have utilized the solar system r- and s- process isotopic abundances of stellar models offered by Arlandini et al. (1999)[200]. The observed elemental abundances are scaled to the metallicity of the corresponding stars and normalized to their respective barium abundances. Elemental abundances are then fitted with the parametric model function $log\epsilon_i = A_s N_{is} + A_r N_{ir}$. The best fit coefficients and reduced chi-square values for the programme stars are given in Table 3.5. While in the case of HD 49641 the observed abundances of neutron-capture elements seem to have similar contribution from s- and r-process, for the objects HD 58368 and HD 191010 contributions from s-process seem to dominate. HD 119650 seem to have more contributions from r-process; this object also shows Sm and Dy with values [X/Fe] $>$ 1.0.

Table 3.5 Best fit co-efficients and reduced chi-square values

Star Name	A_s	A_r	χ^2
HD 49641	0.56 ± 0.10	0.59 ± 0.09	1.71
HD 58368	0.67 ± 0.08	0.25 ± 0.08	0.76
HD 119650	0.39 ± 0.08	0.63 ± 0.07	0.80
HD 191010	0.80 ± 0.08	0.21 ± 0.08	0.95

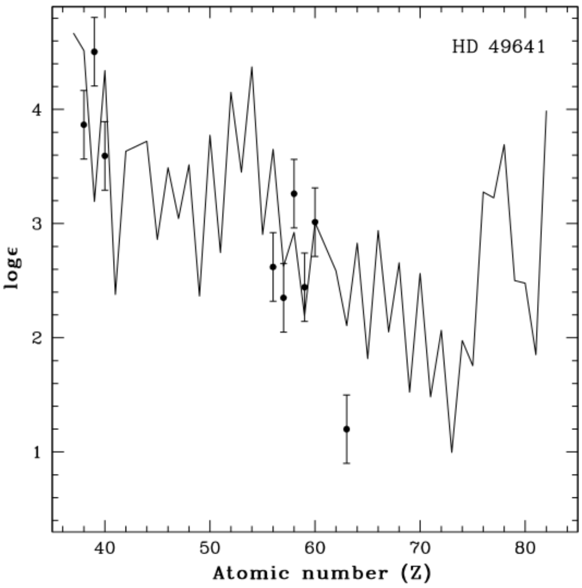

Fig. 3.5 HD 49641

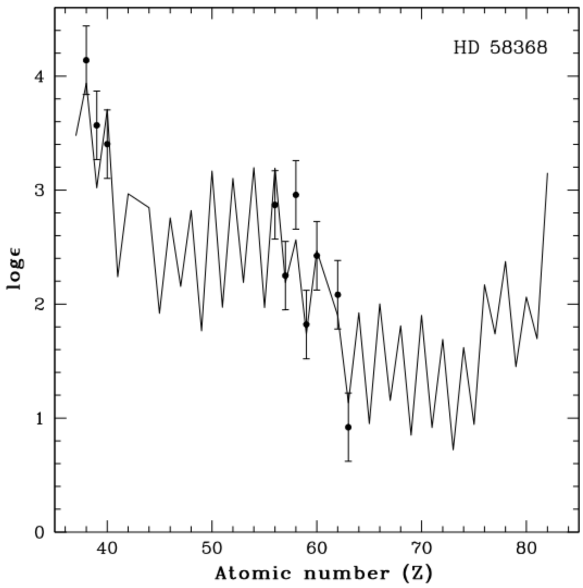

Fig. 3.6 HD 58368

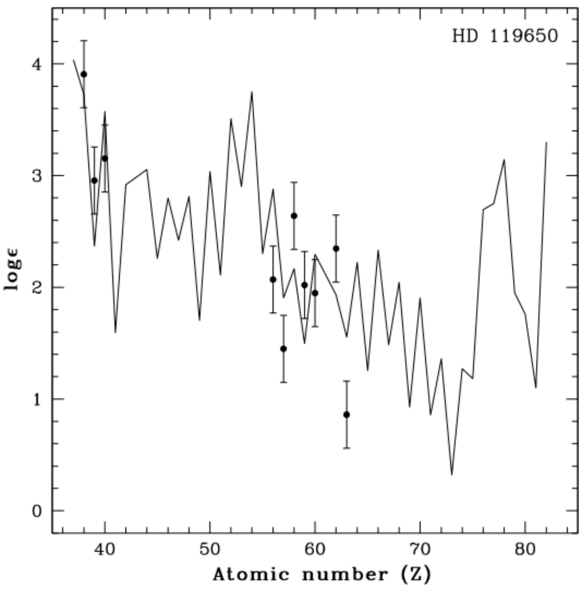

Fig. 3.7 HD 119650

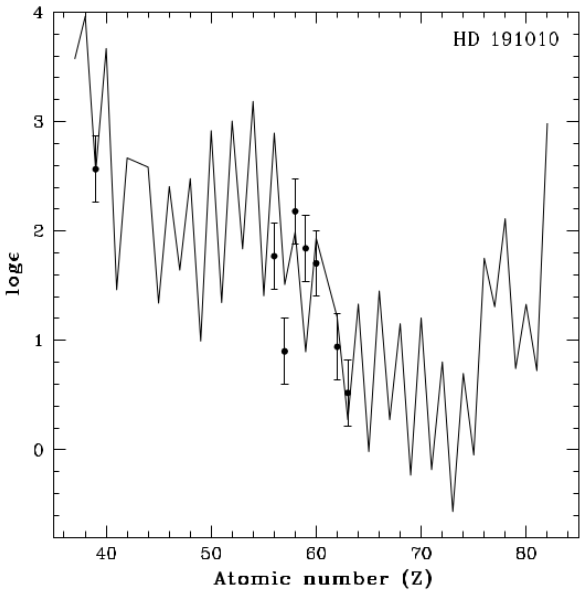

Fig. 3.8 HD 191010

3.7 Summary

Detailed chemical composition studies of stars with enhanced abundances of neutron-capture elements can provide observational constraints for neutron-capture nucleosynthesis studies and clues for understanding their contribution to the Galactic chemical enrichment. We have presented abundance results from high-resolution (R $\sim$ 42000) spectral analyses of a sample of four chemically peculiar stars characterized by s-process enhancement. We report estimates of elemental abundances for several neutron-capture elements, Sr, Y, Zr, Ba, La, Ce, Pr, Nd, Sm, Eu and Dy. While HD 49641 and HD 58368 show [Ba/Fe] $\geq$ 1.16 the other two objects HD 119650 and HD 191010 are found to be mild barium stars with [Ba/Fe] $\sim$ 0.4. The derived abundances of the elements are interpreted on the basis of existing theories for understanding their origin and evolution.